

Pressure Responses of a Vertically Hydraulic Fractured Well in a Reservoir with Fractal Structure*

Kambiz Razminia^a
kambiz.razminia@gmail.com

Abolhassan Razminia^b
razminia@pgu.ac.ir

Delfim F. M. Torres^c
delfim@ua.pt

^a*Department of Petroleum Engineering,
Petroleum University of Technology, Ahwaz, Iran*

^b*Dynamical Systems & Control (DSC) Research Lab., Department of Electrical
Engineering, School of Engineering, Persian Gulf University,
P.O. Box 75169, Boushehr, Iran*

^c*Center for Research and Development in Mathematics and Applications (CIDMA),
Department of Mathematics, University of Aveiro, 3810-193 Aveiro, Portugal*

Abstract

We obtain an analytical solution for the pressure-transient behavior of a vertically hydraulic fractured well in a heterogeneous reservoir. The heterogeneity of the reservoir is modeled by using the concept of fractal geometry. Such reservoirs are called fractal reservoirs. According to the theory of fractional calculus, a temporal fractional derivative is applied to incorporate the memory properties of the fractal reservoir. The effect of different parameters on the computed wellbore pressure is fully investigated by various synthetic examples.

Keywords: vertically hydraulic fractured well; fractal geometry; fractal reservoir; fractional derivatives.

1 Introduction

Hydraulic fracturing plays an important role in improving the productivity of damaged wells and wells producing. The vertical plane fracture is created by injecting fluid into the formation and then filling with propping agents, such as proppants, to prevent closure. In practical terms, two types of fractured well are considered: infinite (high) or finite (low) conductivity vertical fracture. In case of infinite conductivity fracture, it is assumed that the fluid flows along the fracture without any pressure drop. Finite conductivity fracture occurs when the pressure drop along the fracture plane is not negligible.

The classical diffusion equation has been used to explain the pressure responses of a well in a reservoir, which is assumed to be homogenous at all scales. However, recent studies show that the homogeneity assumption is not valid in most cases [1–7]. Due to this fact, fractal geometry has been used as an effective tool to describe the heterogeneities of these reservoirs, which are called fractal reservoirs [8–11]. Since the diffusion process of fractal reservoirs is history dependent, and the anomalous diffusion properties of fractal reservoirs cannot be fully described by the fractal model, the concept of fractional derivative has been used to incorporate the memory of the fluid flow [12–15]. Our main aim here is to analyze the pressure behavior of a well with an infinite

*This is a preprint of a paper whose final and definite form will be published in *Applied Mathematics and Computation*, ISSN: 0096-3003. Submitted 01/July/2014; revised 20/Dec/2014; accepted 29/Dec/2014.

conductivity vertical fracture in a fractal reservoir. An infinite radial system is considered in order to analyze the effects of different parameters on the well response.

The paper is organized as follows. After this brief introduction, the mathematical model is formulated in Section 2. A summary of the nomenclature used appears in Appendix A. The analytical solution to the model is provided in Section 3. Section 4 discusses how the well responses to different reservoir parameters. The main conclusions of our study are given in Section 5.

2 Model description

A schematic diagram of a vertically hydraulic fractured well is shown in Figure 1. Figure 2 shows

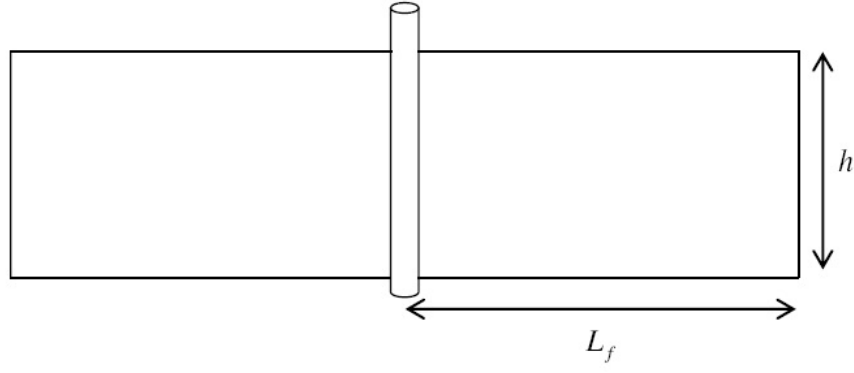


Figure 1: Geometry of a vertically hydraulic fractured well.

the geometry of flow lines near the fractured well. Before discussing the mathematical model of

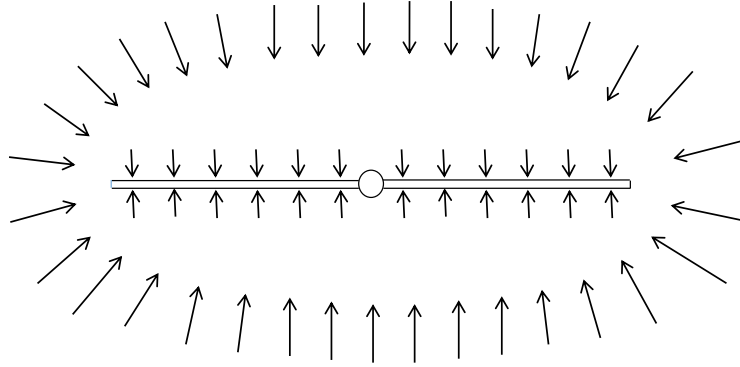


Figure 2: Linear and pseudo-radial flow regimes near an infinite conductivity fracture.

transport process, we define three variables:

- the dimensionless pressure

$$p_D = \frac{2\pi k_w h (p_i - p(r, t))}{q\mu};$$

- the dimensionless time

$$t_D = \frac{k_w r_{wD}^{\theta} t}{\phi_w \mu c (2L_f)^2};$$

- the dimensionless radius

$$r_D = \frac{r}{2L_f}.$$

See Appendix A for the description of all the quantities involved. The best known and most useful model to describe the pressure behavior of fractal reservoirs was firstly proposed by Metzler et al. [1]. Similarly to Camacho-Velázquez et al. [4], from here on we call *generalized diffusion equation* to the fractal-fractional diffusion (FFD) equation

$$\frac{1}{r_D^\theta} \frac{\partial^2 p_D}{\partial r_D^2} + \frac{\beta}{r_D^{\theta+1}} \frac{\partial p_D}{\partial r_D} = \frac{\partial^\gamma p_D}{\partial t_D^\gamma}, \quad (1)$$

where $\beta = d_{mf} - \theta - 1$. The parameter d_{mf} denotes the mass fractal dimension, while θ represents the conductivity index. Mass fractal dimension is responsible for the reservoir structure, and the conductivity index explains the diffusion process in the reservoir. The Caputo fractional order derivative is used to introduce $\partial^\gamma p_D / \partial t_D^\gamma$:

$$\frac{\partial^\gamma p_D}{\partial t_D^\gamma} = \frac{1}{\Gamma(m - \gamma)} \int_0^{t_D} (t_D - \tau)^{m-\gamma-1} p_D^{(m)}(\tau) d\tau, \quad (2)$$

where $\gamma \in \mathbb{R}^+$, $[\gamma] = m \in \mathbb{Z}^+$, and Γ represents the Gamma function, that is,

$$\Gamma(\nu) = \int_0^\infty e^{-\tau} \tau^{\nu-1} d\tau. \quad (3)$$

The order γ of the fractional derivative is related to the conductivity index by $\gamma = 2/(2 + \theta)$.

3 Analytical solution

It is assumed that the pressure distribution of the reservoir is uniform and constant at initial time:

$$p_D(r_D, 0) = 0. \quad (4)$$

To obtain the line source solution of equation (1), we take $r_w \rightarrow 0^+$. The inner boundary condition without wellbore storage and skin effects can then be written as

$$r_D^\beta \frac{\partial p_D(r_D, t_D)}{\partial r_D} \Big|_{r_D \rightarrow 0^+} = -1. \quad (5)$$

The outer boundary condition for the infinite reservoir is given by

$$\lim_{r_D \rightarrow \infty} p_D(r_D, t_D) = 0. \quad (6)$$

Taking the Laplace transform to both sides of (1), and then using (4), we obtain that

$$\frac{1}{r_D^\theta} \frac{\partial^2 \bar{p}_D}{\partial r_D^2} + \frac{\beta}{r_D^{\theta+1}} \frac{\partial \bar{p}_D}{\partial r_D} = s^\gamma \bar{p}_D, \quad (7)$$

where s is the Laplace transform variable. The dependent variable \bar{p}_D denotes the Laplace transform of p_D , and is a function of r_D and s . In the Laplace space, the inner boundary condition takes the form

$$r_D^\beta \frac{\partial \bar{p}_D(r_D, s)}{\partial r_D} \Big|_{r_D \rightarrow 0^+} = -\frac{1}{s} \quad (8)$$

while the outer boundary condition is given by

$$\lim_{r_D \rightarrow \infty} \bar{p}_D(r_D, s) = 0. \quad (9)$$

Using the substitutions $\bar{p}_D = r_D^{(1-\beta)/2} \bar{W}$ and $x = (2s^{\gamma/2} r_D^{(2+\theta)/2})/(2+\theta)$, and after a slight manipulation, we conclude that (7) is equivalent to

$$x^2 \frac{\partial^2 \bar{W}}{\partial x^2} + x \frac{\partial \bar{W}}{\partial x} - (x^2 + \nu^2) \bar{W} = 0, \quad (10)$$

where $\nu = \frac{1-\beta}{2+\theta}$. Equation (10) is Bessel's equation, which has the general solution

$$\bar{W}(x, s) = AI_\nu(x) + BK_\nu(x). \quad (11)$$

Thus, the dimensionless pressure function in Laplace space can be written as

$$\bar{p}_D(r_D, s) = r_D^{(1-\beta)/2} \left[AI_\nu \left(\frac{2s^{\gamma/2}}{2+\theta} r_D^{(2+\theta)/2} \right) + BK_\nu \left(\frac{2s^{\gamma/2}}{2+\theta} r_D^{(2+\theta)/2} \right) \right]. \quad (12)$$

Application of the outer boundary condition (9) to (12) yields $A = 0$. Therefore, (12) reduces to

$$\bar{p}_D(r_D, s) = Br_D^{(1-\beta)/2} K_\nu \left(\frac{2s^{\gamma/2}}{2+\theta} r_D^{(2+\theta)/2} \right). \quad (13)$$

Based on (13), the inner boundary condition (8) can be written as

$$-B \lim_{r_D \rightarrow 0^+} s^{\gamma/2} r_D^{(1+\beta+\theta)/2} K_{\nu-1} \left(\frac{2s^{\gamma/2}}{2+\theta} r_D^{(2+\theta)/2} \right) = -\frac{1}{s}. \quad (14)$$

Equation (14) can be simplified by using the formula

$$K_\nu(x) \approx \frac{\Gamma(\nu)}{2} \left(\frac{2}{x} \right)^\nu, \quad \nu > 0, \quad (15)$$

valid for small arguments $0 < x \ll \sqrt{1+\nu}$. Indeed, having in mind that $K_\nu(x) = K_{-\nu}(x)$, and by making use of (15), we reduce (14) to the following expression:

$$B \lim_{r_D \rightarrow 0^+} s^{\gamma/2} \frac{\Gamma(1-\nu)}{2^\nu} \left(\frac{2+\theta}{2s^{\gamma/2}} \right)^{1-\nu} = \frac{1}{s}. \quad (16)$$

Consequently,

$$B = \frac{2}{\Gamma(1-\nu)(2+\theta)^{1-\nu} s^{1+\nu\gamma/2}}. \quad (17)$$

Equation (13) can be written as

$$\begin{aligned} \bar{p}_D(x_D, y_D, s) &= B \left(\sqrt{(x_D - \alpha_1)^2 + (y_D - \alpha_2)^2} \right)^{(1-\beta)/2} \\ &\quad \times K_\nu \left(\frac{2s^{\gamma/2}}{2+\theta} \left(\sqrt{(x_D - \alpha_1)^2 + (y_D - \alpha_2)^2} \right)^{(2+\theta)/2} \right). \end{aligned} \quad (18)$$

We obtain the pressure drop function, in a fractal reservoir with a hydraulic fracture across the well, by integrating (13) with respect to α_1 from $-1/2$ to $1/2$:

$$\begin{aligned} \bar{p}_{Df}(x_D, y_D, s) &= B \int_{-1/2}^{1/2} \left[\left(\sqrt{(x_D - \alpha_1)^2 + (y_D - \alpha_2)^2} \right)^{(1-\beta)/2} \right. \\ &\quad \left. \times K_\nu \left(\frac{2s^{\gamma/2}}{2+\theta} \left(\sqrt{(x_D - \alpha_1)^2 + (y_D - \alpha_2)^2} \right)^{(2+\theta)/2} \right) \right] d\alpha_1. \end{aligned} \quad (19)$$

Since the computation of the pressure along the fracture is favorable, it can be assumed that $y_D = \alpha_2$. Thus, the pressure drop function (19) reduces to

$$\bar{p}_D(x_D, 0, s) = B \int_{-1/2}^{1/2} \left(\sqrt{(x_D - \alpha_1)^2} \right)^{(1-\beta)/2} K_\nu \left(\frac{2s^{\gamma/2}}{2+\theta} \left(\sqrt{(x_D - \alpha_1)^2} \right)^{(2+\theta)/2} \right) d\alpha_1, \quad (20)$$

where $|x_D| \leq 1/2$. By changing variables, and after further manipulations, (20) can be written as

$$\begin{aligned} \bar{p}_D(x_D, 0, s) = B \frac{1}{s^{\gamma/2}} \left(\frac{2+\theta}{2s^{\gamma/2}} \right)^{a-1} & \left(\int_0^{(2s^{\gamma/2}/(2+\theta))(1/2-x_D)^{(2+\theta)/2}} z^{a-1} K_\nu(z) dz \right. \\ & \left. + \int_0^{(2s^{\gamma/2}/(2+\theta))(1/2+x_D)^{(2+\theta)/2}} z^{a-1} K_\nu(z) dz \right) \end{aligned} \quad (21)$$

with $a = (4 - d_{mf} + \theta)/(2 + \theta)$. The integrals in (21) can be computed by the following formula:

$$\begin{aligned} \int z^{a-1} K_\nu(z) dz = & -\frac{2^{\nu-1} \pi z^{a-\nu} \csc(\pi\nu)}{(\nu-a)\Gamma(1-\nu)} {}_1F_2 \left(\frac{a-\nu}{2}; 1-\nu, \frac{a-\nu}{2} + 1; \frac{z^2}{4} \right) \\ & - \frac{2^{-\nu-1} \pi z^{a+\nu} \csc(\pi\nu)}{(a+\nu)\Gamma(1+\nu)} {}_1F_2 \left(\frac{a+\nu}{2}; 1+\nu, \frac{a+\nu}{2} + 1; \frac{z^2}{4} \right), \end{aligned} \quad (22)$$

where $\nu \notin \mathbb{Z}$ and ${}_1F_2$ represents the generalized hypergeometric function. For the Euclidean model, that is, the particular case $\nu = 0$ and $a = 1$, the presented integrals can be evaluated by

$$\int K_0(z) dz = \frac{\pi z}{2} (K_0(z)L_{-1}(z) + K_1(z)L_0(z)) \quad (23)$$

or

$$\int K_0(z) dz = \frac{\pi z}{2} (K_0(z)L_1(z) + K_1(z)L_0(z)) + zK_0(z), \quad (24)$$

where $L_{-1}(z)$, $L_0(z)$ and $L_1(z)$ are modified Struve functions given by

$$L_\nu(z) = \frac{z^{\nu+1}}{2^\nu \sqrt{\pi} \Gamma(\nu + \frac{3}{2})} {}_1F_2 \left(1; \frac{3}{2}, \nu + \frac{3}{2}; \frac{z^2}{4} \right), \quad -\nu - \frac{3}{2} \notin \mathbb{N}. \quad (25)$$

The inverse transform operation is easily carried out by using the Gaver-Stehfest algorithm [16].

4 Model responses

To show the pressure-transient behavior of a fractured well, we use (21) to compute the wellbore pressure response at $x_D = 0$ (uniform flux solution), without wellbore storage and skin effects. The well intercepts the center of a single vertical fracture plane. According to the uniform flux fracture assumption, the flow rate per unit of fracture surface is constant along the fracture length. Figure 3 shows the different behavior of a well response in a homogenous and fractal reservoir. Generally, the fracture structure works as a sink, which enforces the fluid to go towards the fracture with hyperbolic flow geometry. The geometry of fracture enforces the flow lines to be perpendicular to the fracture plane and the pressure-transient response defines a linear flow in the reservoir. After the linear flow regime, when the effect of fluid flow reaches the two ends of the fracture, the geometry of flow can be identified, for a small time, by a hyperbolic flow regime. Ultimately, the characteristic radial flow regime is observed from the well response. The linear flow regime can be identified by two straight-lines of pressure and its logarithmic derivative at early times (see Figure 3). As can be seen from Figure 3, these two parallel straight-lines have a half slope during the linear flow regime in a conventional reservoir. The specialized analysis (Cartesian coordinates) on Figure 4 shows that with a plot of the pressure change versus the square root

of the elapsed time, the linear flow can be identified with a straight-line intercepting the origin. The results of Figure 4 show that the slope of the straight-line is decreasing with the increasing of the parameter ν . In other words, in a more complex reservoir, described by a larger value of the conductivity index θ and a smaller value of the mass fractal dimension d_{mf} , the linear flow is identified with a smaller slope of the straight-line in the specialized plot. Figure 3 indicates that the radial flow regime (at late times) is identified by the straight-line shape of the logarithmic derivative in log-log scale and that the reservoirs with more complex structures (larger values of ν) have the straight-lines with larger slopes. Moreover, Figure 3 shows that in a fractal reservoir, at late times during the radial flow regime, the pressure response and its logarithmic derivative are parallel straight-lines. This fact indicates that the pressure and its logarithmic derivative can be expressed by two power-law functions with the same power.

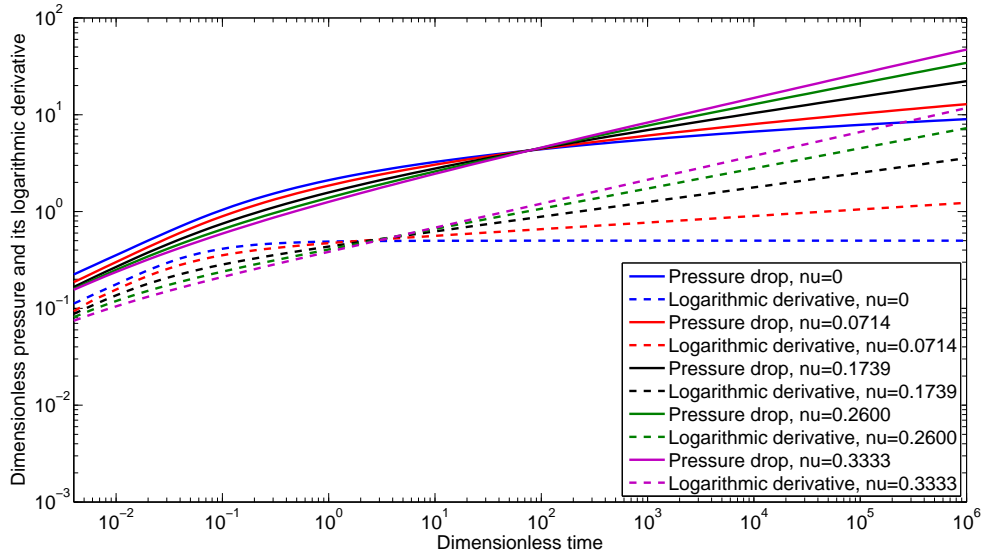


Figure 3: Responses for a fractured well without wellbore storage and skin effects. Log-log analysis of p_D and $dp_D/d\ln(t_D)$ versus t_D with $d_{mf} = \{2, 1.95, 1.9, 1.85, 1.8\}$, $\theta = \{0, 0.1, 0.3, 0.5, 0.7\}$ and $\gamma = \{1, 0.9524, 0.8696, 0.8000, 0.7407\}$.

The reservoir rock porosity is a statistical property of the system, and can be expressed as $\phi(r) = \phi_r(r/L_r)^{d_{mf}-2}$, where ϕ_r is a reference porosity value at the reference length L_r . Particularly, the reference length is the wellbore radius, and the porosity of a fractal reservoir can be written as $\phi(r) = \phi_w(r/r_w)^{d_{mf}-2}$. The reference porosity value can be assumed to be equal to the porosities obtained from log and core data. However, based on log and core porosities, the reasonable oil-in-place estimates indicate that the porosity variations are not big, and can be considered equal to the constant reference porosity. It can be therefore immediately concluded that the mass fractal dimension d_{mf} is equal to the Euclidean dimension, that is, $d_{mf} = 2$. On the other hand, because $k(r) = k_r(r/L_r)^{d_{mf}-\theta-2}$ and, particularly, $k(r) = k_w(r/r_w)^{d_{mf}-\theta-2}$, the deficiencies of average permeability calculations indicate that the dynamical properties of the system have an important role in the flowing fluid through the reservoir and in all stages of production. Since $d_{mf} = 2$, the permeability variations can be expressed by $k(r) = k_w(r/r_w)^{-\theta}$. So, it requires investigating the effect of the conductivity index θ variations on the well response. As can be seen from Figure 5, by increasing the θ values, the pressure responses and their logarithmic derivatives increase. For a constant-rate production, more pressure drops in reservoirs with a more complicated diffusion process (larger θ) indicates that the diffusion is slower in these types of reservoirs. Therefore, application of the conventional model solutions to such reservoirs may lead the analyst

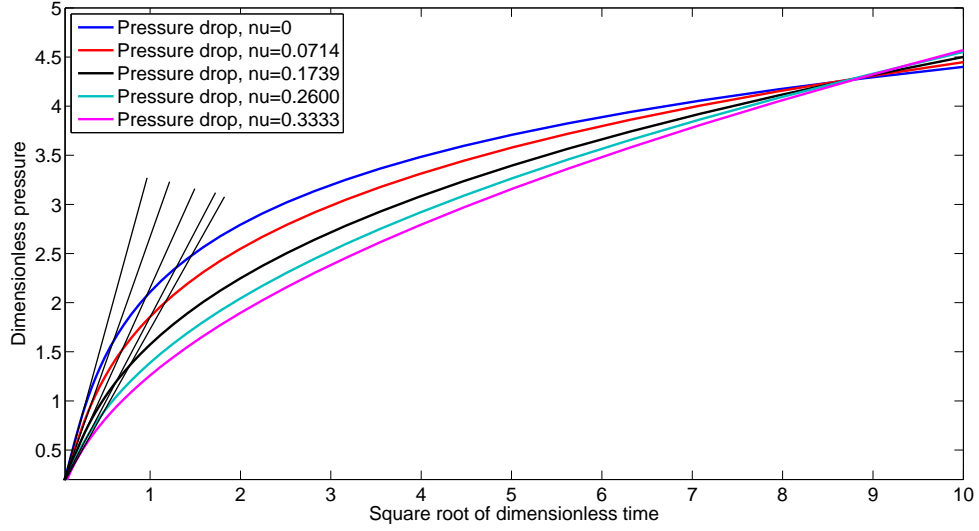


Figure 4: Specialized analysis of p_D versus $\sqrt{t_D}$ with $d_{mf} = \{2, 1.95, 1.9, 1.85, 1.8\}$, $\theta = \{0, 0.1, 0.3, 0.5, 0.7\}$ and $\gamma = \{1, 0.9524, 0.8696, 0.8000, 0.7407\}$.

to a wrong interpretation.

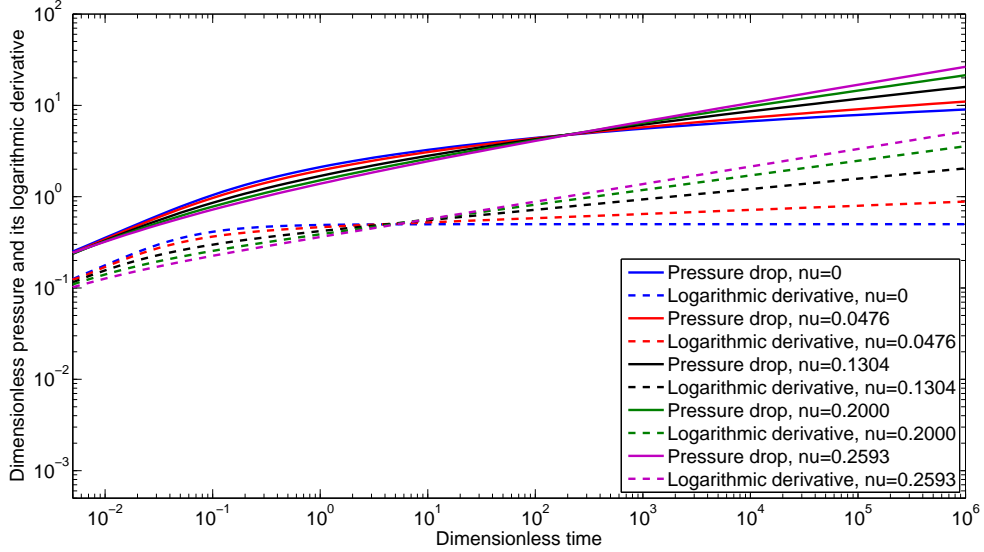


Figure 5: Responses for a fractured well without wellbore storage and skin effects. Log-log analysis of p_D and $dp_D/d\ln(t_D)$ versus t_D with $d_{mf} = 2$, $\theta = \{0, 0.1, 0.3, 0.5, 0.7\}$ and $\gamma = \{1, 0.9524, 0.8696, 0.8000, 0.7407\}$.

5 Concluding remarks

We used fractional calculus to model an infinite conductivity vertically fractured well in a fractal reservoir with more realistic behavior than the conventional (homogeneous) reservoirs. An analytical solution was obtained, allowing us to analyze and interpret the well test data taken from these types of wells and reservoirs. On the basis of our results, the simulated examples and the discussion presented, the following conclusions can be expressed:

- the Euclidean interpretation model cannot be used to analyze the pressure-transient behavior of fractal reservoirs;
- the obtained solution can be used as a practical tool to analyze the effects of dynamical properties of the system;
- according to the shortcomings of the average permeability estimates, the analytical solution can be used to determine the conductivity index parameter θ and then the permeability variations.

A Nomenclature

Symbol	Meaning	Units
c	compressibility	vol/vol/atm
d_{mf}	mass fractal dimension	
${}_1F_2$	generalized hypergeometric function	
h	reservoir thickness	cm
I_ν	modified Bessel function of the first kind of order ν	
k	permeability	darcy
k_w	permeability at the wellbore	darcy
K_ν	modified Bessel function of the second kind of order ν	
L_f	fracture half-length	cm
L_ν	modified Struve function of order ν	
p	pressure	atm
p_D	dimensionless pressure	
p_i	initial pressure	atm
q	production rate	cc/sec
r	radial distance	cm
r_D	dimensionless radius	
r_w	wellbore radius	cm
r_{wD}	dimensionless wellbore radius	
t	time	sec
t_D	dimensionless time	
s	Laplace image space variable	
γ	fractional derivative order	
Γ	Gamma function	
θ	conductivity index	
μ	viscosity	cP
ϕ	porosity (or void fraction)	
ϕ_w	porosity at the wellbore	

Acknowledgments

This work was partially supported by CIDMA & FCT within project PEst-OE/MAT/UI4106/2014.

References

- [1] Chang J, Yortsos YC. Pressure-transient analysis of fractal reservoirs. *SPE Formation Eval* 1990;5:31–38.
- [2] Acuna JA, Ershaghi I, Yortsos YC. Practical application of fractal pressure transient analysis of naturally fractured reservoirs. *SPE Formation Eval* 1995;10:173–179.
- [3] Yao Y, Wu YS, Zhang R. The transient flow analysis of fluid in a fractal, double-porosity reservoir. *Transport Porous Med* 2012;94:175–187.
- [4] Camacho-Velázquez R, Fuentes-Cruz G, Vásquez-Cruz M. Decline-curve analysis of fractured reservoirs with fractal geometry. *SPE Reserv Eval Eng* 2008;11:606–619.
- [5] Yang F, Ning Z, Liu H. Fractal characteristics of shales from a shale gas reservoir in the Sichuan Basin, China. *Fuel* 2014;115:378–384.
- [6] Sheng CC, Zhao JZ, Li YM, Li SC, Jia H. Similar construction method of solution for solving the mathematical model of fractal reservoir with spherical flow. *J Appl Math* 2013; Art. ID 219218, 8 pp.
- [7] Razminia K, Razminia A, Baleanu D. Investigation of fractional diffusion equation based on generalized integral quadrature technique. *Appl Math Model* 2015;39:86–98.
- [8] Acuna JA, Yortsos YC. Application of fractal geometry to the study of networks of fractures and their pressure transient. *Water Resources Res* 1995;31:527–540.
- [9] Cossio M, Moridis GJ, Blasingame TA. A semianalytic solution for flow in finite-conductivity vertical fractures by use of fractal theory. *SPE J* 2013;18:83–96.
- [10] Li W, LI Xp, LI Sc, LI Qy. The similar structure of solutions in fractal multilayer reservoir including a quadratic gradient term. *J Hydrodyn, Ser. B.* 2012;24:332–338.
- [11] Razminia K, Razminia A, Trujillo JJ. Analysis of radial composite systems based on fractal theory and fractional calculus. *Signal Processing* 2015; 107:378–388.
- [12] Metzler R, Glöckle WG, Nonnenmacher TF. Fractional model equation for anomalous diffusion. *Physica A* 1994;211:13–24.
- [13] Razminia K, Razminia A, Machado JAT. Analysis of diffusion process in fractured reservoirs using fractional derivative approach. *Commun. Nonlinear. Sci. Numer. Simulat.* 2014;19:3161–3170.
- [14] Park HW, Choe J, Kang JM. Pressure behavior of transport in fractal porous media using a fractional calculus approach. *Energ Source* 2000;22:881–890.
- [15] Raghavan R. Fractional derivatives: Application to transient flow. *J Petrol Sci Eng* 2011;80:7–13.
- [16] Gaver DP Jr. Observing stochastic processes and approximate transform inversion. *Oper Res* 1966;14:444–459.